



NUMERICAL INVESTIGATION ON ENGINE INLET DISTORTION UNDER CROSSWIND FOR A COMMERCIAL TRANSPORT AIRCRAFT

Kaili Liu ^{*}, Yifeng Sun ^{*}, Yuan Zhong ^{*}, Huiliu Zhang ^{*}, Kunyuan Zhang [†], Hui Yang ^{*}

^{*} Shanghai Aircraft Design and Research Institute, COMAC, Shanghai, China

[†] Nanjing University of Aeronautics and Astronautics, Nanjing, China

Keywords: *total pressure distortion, inlet, numerical simulation, crosswind*

Abstract

Inlet distortion can cause a decrease in the performance of the commercial transport aircraft engines due to the stall and instability which would have significant impact to the economy and safety of the aircraft.

Inlet distortion under crosswind for a high bypass ratio turbofan engine is numerically simulated motivated by the need of engine/airframe integration of a commercial transport aircraft. The inlet flow field, characteristics and underlying flow physics are investigated. The investigation suggests that: A sudden increase in the distortion index occurs as the onset of the internal flow separation; Inlet distortion will deteriorate with increasing crosswind speed. Flow separations, reattachments and ground vortex are found to be the root causes for the crosswind distortion. When ground effect is taken into account, it will lead to inlet distortion and its effect will intensified with higher crosswind. The tolerance of crosswind would be reduced as the flowfield affected by the ground vortex phenomenon. The results and methods provide credibility which will technically benefit the engine/airframe integration, experiments as well as corresponding flight tests.

1 General Introduction

An inlet/nacelle should be designed to meet the requirements of the engine and the aircraft ^[1-2], including satisfying the engine flow requirement, minimizing the weight/drag and the noise, and

maximizing flow quality. The distortion of inlet is a key parameter to evaluate the quality of supplied airflow, which directly related to the engine performance. The consequence distortion would affect the engine stability, the economy and security of commercial transport aircraft.

The crosswind is a typical condition leads to the inlet distortion. In the aircraft airworthiness regulations: the engine must supplied with sufficient amount of airflow in the certification; none adverse characteristics such as stall, surge or flameout appeared during operation; none harmful vibration caused by the flow distortion during operation ^[3]. Many tests and numerical simulations about the inlet distortion were focused on the performance of inlet ^[4-7]. Investigations about inlet distortion with crosswind are studied with wind tunnel experiments and flight tests to provide evidence for the safe operation under crosswind. However, experiments and tests are not only cost much, but unable to obtain details of the flow characteristics and mechanism to integrate engine and aircraft. Numerical simulations have become an economic but effective method to investigate inlet distortion with crosswind in recent years. In order to analyze the performance of civil aircraft inlet, L. Tourrette developed numerical methods and turbulence models, based on the numerical solution of the Navier-Stokes equations, were verified by tests ^[8]. Luis G. T. researched the inlet distortion of a civil aircraft with crosswind by numerical simulation, concluded that the inlet distortion exacerbated by the phenomenon of ground

vortex [9]. In order to build an efficient but robust platform to predict the inlet distortion, Y. Colin carried out some numerical simulations about the inlet distortion [10].

In this paper, a typical large bypass ratio engine inlet flow field is numerical investigated for a commercial transport aircraft. The characteristics and the mechanism of the inlet distortion with large crosswind are studied, which is motivated by the need of the integration research about engine and aircraft. The ground vortex effect is comprehensively taken into account for the interference to flow mechanism of the inlet distortion. The results and research methods in this paper provide credibility for current work, which will technically benefit the engine/airframe integration and its performance tests as well as future corresponding flight tests.

2 Numerical method and conditions

2.1 Computational setup

The CFD simulations are performed using ANSYS CFX solver, which is based on the finite volume method. With the aid of the full-implicit time discretization and the high-order upwind scheme, the three-dimensional Reynolds-averaged Navier-Stokes and two-equation SST $k-\omega$ turbulence model are solved. The residuals and flow are monitored in the calculation until the residuals dropped below four orders of magnitude or remain stable.

Corresponding boundary condition of Inlet and Outlet are set for the computational domain as shown in Figure 1, and the free stream temperature, pressure, velocity, etc. are specified as the input parameters. It should be noticed that the accuracy of the result is also determined by the simplified boundary condition model of the nacelle. As shown in Figure 1, the nacelle exit of the inlet namely fan plane is set to OUTLET boundary condition. The parameters at the OUTLET such as pressure, temperature and velocity are derived by the corrected mass flow, mass flow rate (Φ), total pressure recovery, etc. of the engine operating state, while:

$$\varphi(M_2) = \frac{\Phi \rho_\infty V_\infty A_1 \sqrt{T_\infty^*}}{KA_2 \sigma p_\infty^*} \quad (1)$$

Or,

$$\varphi(M_2) = \frac{W}{241.266 A_2} \quad (2)$$

$$p_2 = \sigma p_\infty^* \left(1 + \frac{k-1}{2} M_2^2 \right)^{\frac{k}{k-1}} \quad (3)$$

$$T_2 = T_\infty^* \left(1 + \frac{k-1}{2} M_2^2 \right) \quad (4)$$

At the exit plane of the nacelle, inflow is set as the INLET boundary condition, and the parameters are specified according to the captured airflow and free stream total temperature. The exposed surfaces of the nacelle are specified as no-slip WALL boundary condition. When the ground effect is taking into account, the ground is set to no-slip WALL boundary condition as the aircraft is at static condition.

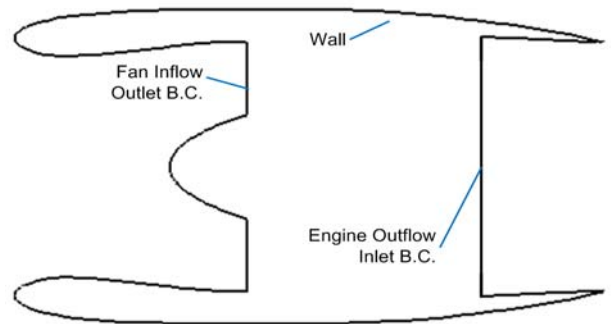


Fig.1 Boundary conditions around the nacelle

2.2 Calculation condition

The inlet distortion at takeoff condition is analyzed. The takeoff calculation is conducted at sea level of international standard atmosphere conditions for a commercial transport aircraft: Flight height of 0.0m, static temperature of 288.15K, and static pressure of 101325.0Pa. The corrected mass flow is 547.8kg/s of the engine at takeoff.

The angle of attack of the nacelle is 0.0°, and the angle of sideslip is 90.0°. The interference of installation angle and body/wing/lift device to the nacelle inlet airflow is not taken into account.

2.3 Analysis method of distortion

There are different rules to evaluate the flow distortion. The form of distortion index chosen to evaluate the flow quality at the exit of the inlet on specific condition is related to some experiences and traditions. In order to quantitative measure the flow distortion, circumferential distortion index (IDC) and radial distortion index (IDR) are adopt according to the requirements of engine supplier and worthiness. The definition of IDC and IDR are shown as follows:

$$IDC = \frac{P_{ring-av} - P_{ring-min}}{P_{av}} \quad (5)$$

$$IDR = \frac{P_{av} - P_{ring-av}}{P_{av}} \quad (6)$$

The method to calculate the distortion index in this paper is entirely consistent with the measurement method of the related wind tunnel experiments. That is sampling a series of monitoring points which are selected regularly along circumferential orientation and radial orientation at fan plane, and the aerodynamic parameters are calculated to acquire the distortion based on the result of CFD. The results in this paper show that the proposed method has certain accuracy to evaluate inlet distortion at crosswind conditions.

2.4 Verification of solver

In order to verify the solver for nacelle flow field, TPS (turbine powered simulator) wind tunnel test data [11] of 'NAL-AERO-02-01' and three dimensional numerical results are compared. For the verification, the free stream Mach number adopted of the tests is 0.602, and the mass flow rate is 0.496. NPR (Nozzle Pressure Ratio) of the TPS fan nozzle is 1.54, and the NPR of the TPS primary nozzle is 1.13. The comparison between the numerical results and experimental data of the pressure coefficient at fan cowl and core cowl are presented in Figure 2. It is worth noting that the calculated results shows good agreement with

the experimental data, which means that the calculation method, mesh, model and the boundary condition presented in this paper are appropriate for the simulation of flowfield of nacelle for aircraft.

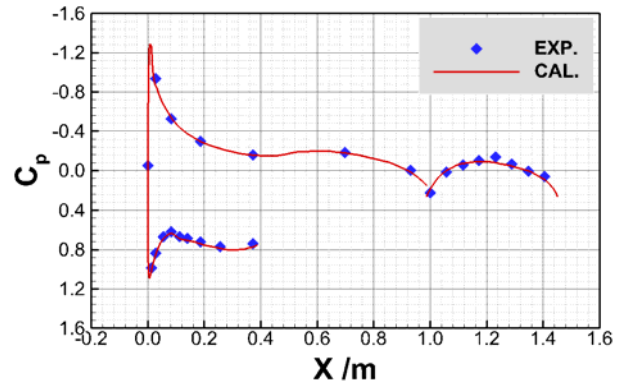


Fig.2 Pressure distribution on the symmetric surface of TPS

3 Isolated nacelle cases

3.1 Nacelle model

A typical commercial transport aircraft engine nacelle is studied and inlet distortion at crosswind is researched. Figure 3 shows the schematic diagram of assembled model of the nacelle model, including the inlet, fan cowl, cone and the nozzle system. Since the main concern of this paper is the aerodynamic characteristics of the inlet, nacelle model is simplified appropriately. The simplification is only about exhaust system, while the inlet, fan cowl and cone remain consistent with the original model of the nacelle.

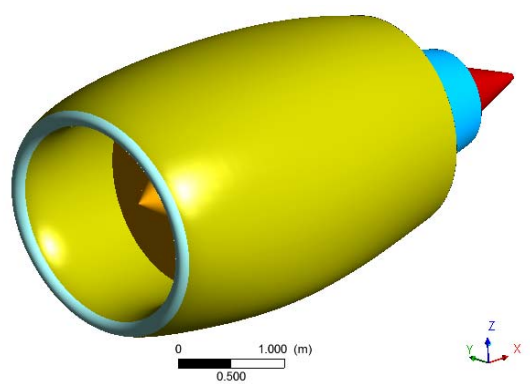


Fig.3 Schematic diagram of nacelle

3.2 Computational mesh

Three dimensional structured mesh of nacelle for computation is generated by ANSYS ICEM CFD software. Figure 4 is a sketch map of the mesh on the nacelle. In order to ensure the accuracy of the calculation results, the upstream far field is extended to a distance of 15 times of the nacelle diameter, while the downstream border mesh is extended to a distance of 30 times of the nacelle diameter to capture jet and mixing flow accurately. The grid near the wall of nacelle is refined to capture flow features in the boundary layer. The structure mesh is refined towards the wall and the smallest mesh height is 0.05 mm to ensure the y^+ near the wall around. Additionally, appropriate refinement is used in the area where the flow changes dramatically, such as the inlet, lip and exhaust system. There are about 3.5 million cells over the three-dimensional flow field. It should be noticed that the structured mesh for the nacelle with the ground is generated when the ground effect is concerned. The height between the ground and the inlet/nacelle is based on the actual height above ground of certain civil aircraft engine. The mesh topology and refinement of the nacelle core with the ground condition is the same as the earlier one, also the mesh near the ground is refined particularly.

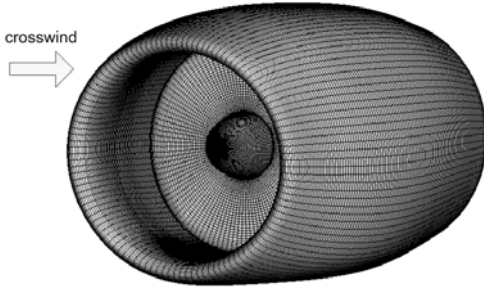


Fig.4 Computational grids on the nacelle surface

3.3 Discussion

According to the civil aircraft operational requirements, the inlet should be designed to meet the inflow quality requirements under the crosswind no less than 20 kt (about 10.29m/s). Of the first, the influence of crosswind speed on the inlet distortion is studied under the

validation operating conditions of the engine. The crosswind speed is about 10 ~ 35 kt.

Figure 5 shows the total pressure recovery (σ) distribution on the fan plane at different crosswind velocity of 15, 20, 25 and 30 kt. In the Figure 5, the total pressure recovery coefficient distributions at crosswind velocity of 15, 20 and 30 kt are similar. And the lower value regions which lead to the distortion increased are mostly near the wall which is apparently due to the viscosity of flow near the wall results in total pressure deduction. While the crosswind velocity increased to 30 kt, there is a lower total pressure region appeared near the 45°, the definition of the location is shown in Figure 6, which locate at the upwind of fan plane, and this region leads to the inlet distortion increased notability.

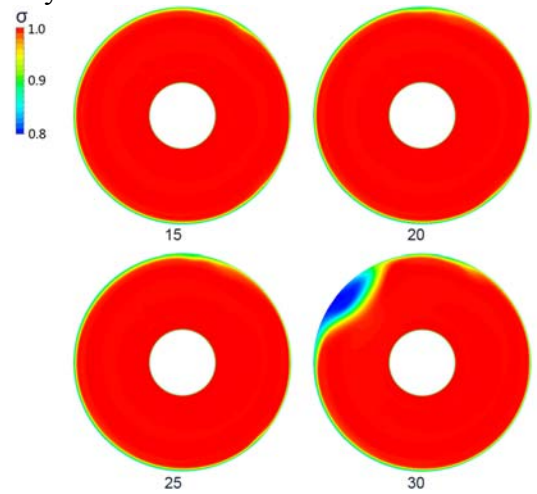


Fig.5 Total pressure contours on the fan plane
(w/o. ground)

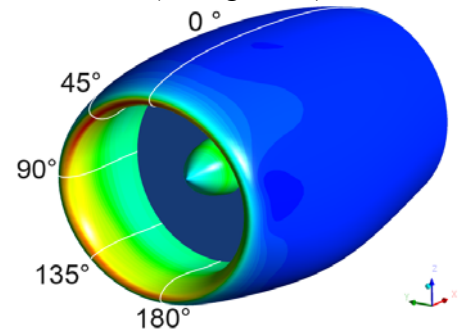
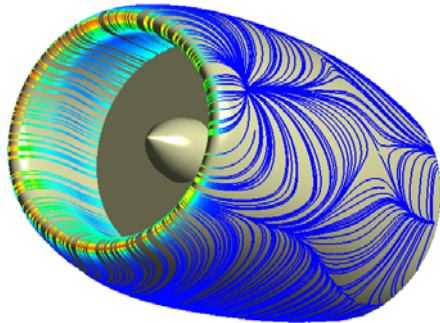


Fig.6 Circumferential cut sections definition

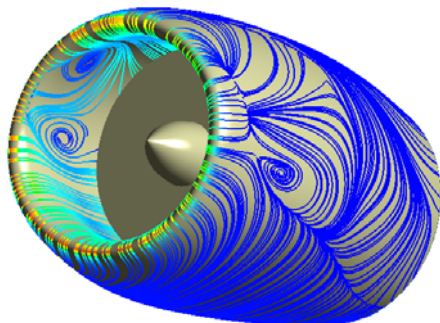
Surface streamlines on the nacelle at the crosswind velocity of 20 kt and 30 kt are shown

NUMERICAL INVESTIGATION ON ENGINE INLET DISTORTION UNDER CROSSWIND FOR A COMMERCIAL TRANSPORT AIRCRAFT

in Figure 7 (a) and (b) respectively. It is observed that the internal flow field characteristics varies greatly with the crosswind velocity increasing from 20 kt to 30 kt. There are two separate vortexes appeared around 45° location as the crosswind velocity is 30 kt. The separate vortex is the main factor results in the intensify loss of total pressure. It is obviously that the mechanism of distortion is the increase of the crosswind speed which cause large internal flow separation gradually extends.



(a) 20 kt

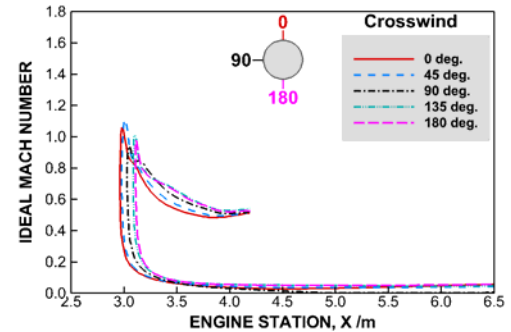


(b) 30 kt

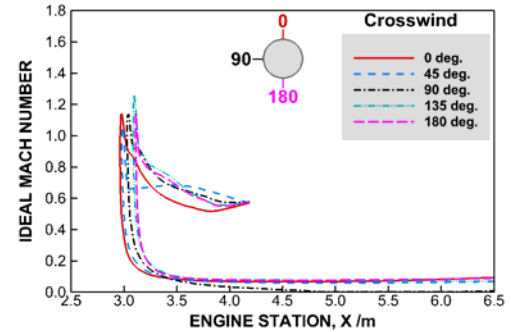
Fig. 7 Surface streamline of nacelle

In order to study the mechanism of flow separation, the isentropic Mach distributions on the nacelle wall under crosswind velocity of 20 kt and 30 kt are illustrated in Figure 8. The dimensionless parameter of isentropic Mach number is calculated by local pressure and free stream total pressure. The total pressure loss caused by the viscosity is ignored in the isentropic Mach number calculation. The results at the direction of 0°, 45°, 90°, 135°and 180°are illustrated in the Figure 8. It can be seen the

Max isentropic Mach number in the direction of 45° near the lip of the nacelle is up to 1.1, which is caused by the accelerating of the captured inflow by the engine. In order to satisfy the performance requirement at low speed, the civil aircraft inlets are preferred to be designed with a thick lip at the direction from 180° to 90°. In corresponding is that the surface curvatures at these locations are small, which make the airflow near the wall accelerate slowly and the peak Isentropic Mach number decrease. However, the inlets are designed with a thin lip at the 0° direction. The airflow near the wall at the direction from 0° to 90° accelerate fast and reach a high peak isentropic Mach number. The integrated influence of the adverse pressure gradient and high peak isentropic Mach number near the throat leads to flow separation under the crosswind velocity of 30 kt and the inflow distortion would increase.



(a) 20 kt



(b) 30 kt

Fig. 8 Wall isentropic Mach distributions(w./o. ground)

It also can be concluded that the performance of the nacelle/inlet scheme can satisfy the air quality requirements under the crosswind at 20 kt.

For aircraft taking off or landing at crosswind conditions, it will be affected by the ground effect. When engine aerodynamic performance is tested in wind tunnel, the ground effect also needs to be simulated to quantify its impact. In this paper, CFD simulations considering ground effect are conducted with the isolated engine model. Assuming the same crosswind speeds, inlet mass flow rate, a comparison study for engine inlet distortion is performed. The inlet total pressure recovery is compared in Figure 9 with crosswind speeds at 15, 20, 25, 30 kt respectively. No significant differences are discovered below 25 kt at high total pressure region. When the crosswind increase from 25 kt to 30 kt, low total pressure occurs at 45 degrees on fan plane in the windward side like results depicted before, which represents a more severe distortion.

When ground effect is taken into account, a low total pressure region appears under the same crosswind speed (Figure 5 and Figure 9). Total pressure and Q criterion contour at 20, 25, 30 and 35 kt are further given in Figure 10. A ground vortex is formed on the ground and ingested into the engine inlet^[12-15], which can interpret the low pressure region. In Figure 9, when the crosswind speed increased from 15 kt to 30 kt, the ground vortex increased its strength and the inlet distortion deteriorates. It is noted that when the crosswind is at 30 kt, windward flow separation again appears at 45 degrees. The formation and development of engine ground vortex is determined by parameters like inlet mass flow rate, distance to ground, crosswind speed and etc. When crosswind speed attains 35 kt, stream tube captured by the inlet is narrowed down and its interaction with ground is reduced, engine ground vortex finally disappears.

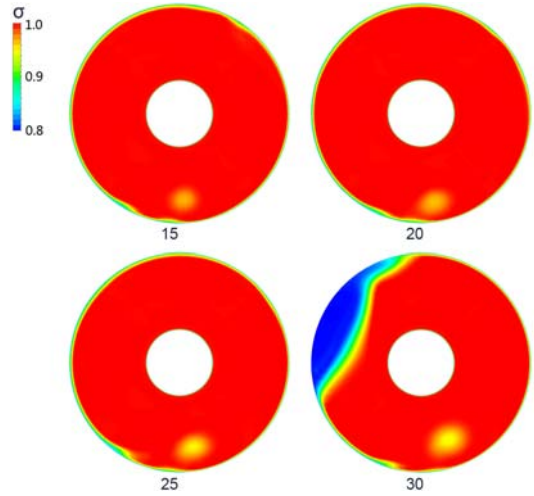


Fig.9 Total pressure contour on fan plane(with ground)

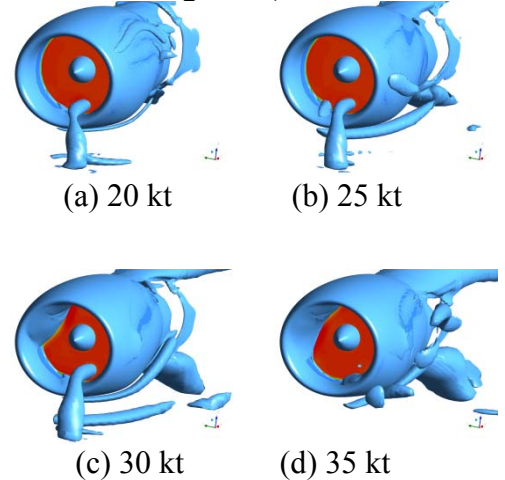


Fig.10 Total pressure contour and Iso-surface with $Q=2500$

To quantify the inlet distortion, circumferential distortion index (IDCmax) against wind speed is provided in Figure 11 with and without ground effect. IDCmax agrees well for wind speed below 26 kt. Owing to the ground vortex, IDCmax increases a bit when ground effect is included. It is noted that with ground effect IDCmax exceeds engine performance SPEC at 26 kt, which is 3 kt lower than the case without ground.

NUMERICAL INVESTIGATION ON ENGINE INLET DISTORTION UNDER CROSSWIND FOR A COMMERCIAL TRANSPORT AIRCRAFT

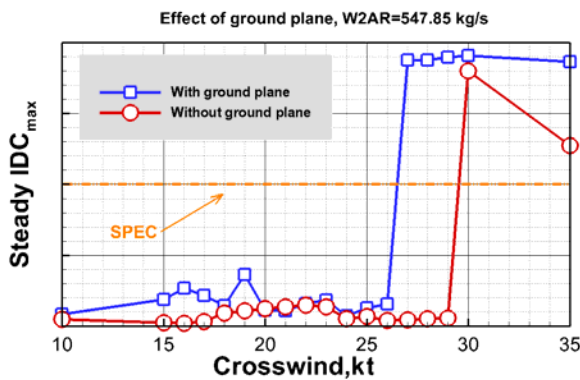


Fig.11 Variation of IDC_{max} with crosswind speed

Under the same engine operation condition, distinct flow features are demonstrated with and without considering ground effects. Engine ground vortex produces lower density around vortex core, which leads to increased mass flow in other regions to meet the total mass flow requirements of the engine. Isentropic Mach number distribution at 20 kt and 30 kt crosswind speed are given in Figure 12. The Isentropic Mach number increases from 1.1 to 1.4 close to the inlet lip at 45 degree. Higher adverse pressure gradient will cause the incoming flow more prone to separation and sudden incensement of IDC_{max} . After the inlet flow separates, Isentropic Mach number distribution at 45 degree will not change any more. At the speed of 30 kt, the maximum Mach number close to the leading edge is around 1.2 at 135 degree (Figure 12(b)).

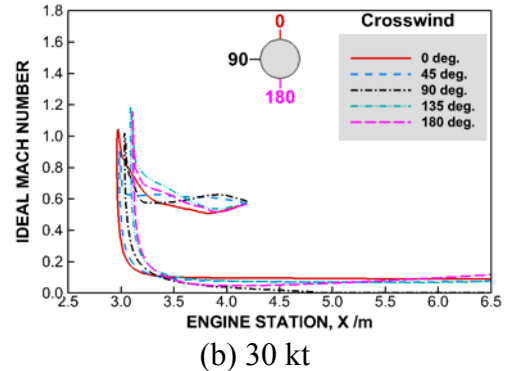


Fig.12 Wall isentropic Mach distributions(with ground)

4. Conclusion

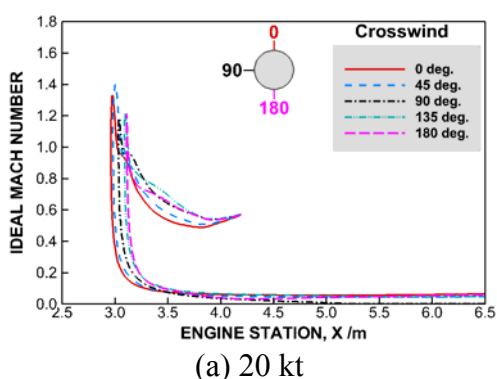
Aerodynamic characteristics of inlet distortion under crosswind for a commercial transport aircraft are investigated numerically. Some conclusions can be drawn as follows:

(a) An isolated nacelle model is used to study the effect of increasing crosswind on inlet distortion. It is noticed that the flow separations, reattachments and ground vortex are the root cause for the crosswind distortion.

(b) The onset of the internal flow separation and the loss of total pressure lead to a sudden increase in the distortion index at the fan plane. Flow separations continue to develop with increased crosswind speed and dominate the inlet distortion.

(c) When the ground effect is taken in account for the isolated nacelle model, a low total pressure region appears under the same crosswind speed and the inlet distortion deteriorates. The ground vortex becomes a primary cause for the crosswind distortion. It should be noticed that the tolerance of crosswind would be reduced as the nacelle flowfield affected by the ground vortex phenomenon.

Preliminary simulations are completed and further investigations are needed to profoundly understand the inlet distortion under crosswind. The wing, lift device and fuselage with the ground are going to be taken into account in the



(a) 20 kt

future investigations for the interference to flow mechanism of the inlet distortion.

References

- [1] ZHAO He-shu. Aircraft inlet aerodynamic principles. *National defense industry press*, 1989. (in Chinese)
- [2] J. Seddon, E.L. Goldsmith. Intake aerodynamics 2nd.*AIAA education series*, 1999.
- [3] Chen Da-guang, Zhang Jin. Optimization of Aircraft-Engine matching performance. *Beijing university of aeronautics and astronautics press*, 1990. (in Chinese)
- [4] A. L. Schuehle. 727 Airplane side inlet low-speed performance confirmation model test for refanned JT8D engines. *NASA*, No. CR-134609, 1974.
- [5] J.P.HANCOCK, B.L. HINSON. Inlet development for the L-500. *AIAA Paper*, No. 69-448, 1969.
- [6] C. A. Hall, T. P. Hynes. Measurements of intake separation hysteresis in a model fan and nacelle rig. *AIAA Paper*, No. 2002-3772, 2002.
- [7] ZUO Zhi-cheng, QIAN Rui-zhan. Numerical simulation investigation of effect of thrust-reverser operating on engine inlet flow distortion for civilian transport. *Aircraft design*, Vol. 27, No. 5, pp 60-64, 2007.(in Chinese)
- [8] Tourrette, L. . Navier-Stokes simulations of air-intakes in crosswind using local preconditioning. *AIAA Paper*, No.2002-2739, 2002.
- [9] Luis Gustavo Trapp, Roberto da motta Girardi. Evaluation of engine inlet vortices using CFD. *AIAA Paper*, No. 2012-1200, 2012.
- [10]Y. Colin, B. Aupoix, J. F. Boussuge, P. Chanez. Numerical simulation of the distortion generated by crosswind inlet flows. *ISABE*, No. 2007-1210, 2007.
- [11]Hirose N, Asai K, Ikawa K. Transonic 3D Euler analysis of flows around fan-jet engine and T.P.S. (turbine powered simulator). *NAL-TR-1045*, 1989.
- [12]Johns, C. J. . The aircraft engine inlet vortex problem. *AIAA Paper*, No. 2002-5894, 2002.
- [13]Trapp, L. G., & Motta Girardi, R. D. . Crosswind effects on engine inlets: The inlet vortex. *Journal of aircraft*, Vol. 47, No. 2, pp 577-590, 2010.
- [14]Yoram Yadlin, Arvin Shmilovich. Simulation of vortex flows for airplanes in ground operations. *AIAA Paper*, No.2006-56, 2006.
- [15]Nathan Rosendo Horvath. Inlet vortex formation under crosswind conditions. *Worcester: Worcester polytechnic instititure*, 2013.

Copyright Statement

The authors confirm that they, and/or their company or organization, hold copyright on all of the original material included in this paper. The authors also confirm that they have obtained permission, from the copyright holder of any third party material included in this paper, to publish it as part of their paper. The authors confirm that they give permission, or have obtained permission from the copyright holder of this paper, for the publication and distribution of this paper as part of the ICAS 2014 proceedings or as individual off-prints from the proceedings.

5 Contact Author Email Address

The contact author email address, mail to:
liukaili@comac.cc